Calcium uptake hotspots in the mitochondria of cardiac muscle at the interface with dyadic SR

Sergio De La Fuente[1], Celia Fernandez-Sanz[4], Caitlin Vail[1], Elorm J. Agra[1], Kira Holmstrom[2], Junhui Sun[3], Jyotsna Mishra[4], Toren Finkel[2], Elizabeth Murphy[3], Suresh K. Joseph[1], Shey-Shing Sheu[4], György Csordás[1]

[1]MitoCare Center, Pathology, Anatomy & Cell Biology, Thomas Jefferson University, Philadelphia, PA, USA, [2]Center for Molecular Medicine, Lab. of Molecular Biology, NIH-NHLBI, Bethesda, MD, USA
[3]Systems Biology Center, Laboratory of Cardiac Physiology, NIH-NHLBI, Bethesda, MD, USA, [4]Center for Translational Medicine, Thomas Jefferson University, Philadelphia, PA, USA

INTRODUCTION

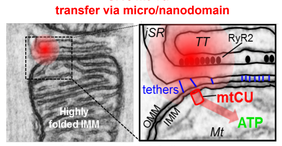

mtCU, mitochondrial Ca^{2+} uniporter = MCU (pore) + MICUs (Ca^{2+} sensors) + EMRE (essential TM component) + other regulators (MCUb, MCUR1)

- Control of the mitochondrial ATP production by SR-derived Ca^{2+} signals includes local, nanodomain Ca^{2+} transfer from ryanodine receptors (RyR2) to the mitochondrial matrix (excitation-bioenergetics coupling).
- Ca^{2+} crosses the inner mitochondrial membrane (IMM) via the mtCU, a low-affinity Ca^{2+}-activated Ca^{2+} channel complex.
- The surface area of cardiac IMM is extensively enhanced by cristae folding; however, mitoplast patch clamp studies showed mtCU current density the lowest amongst a range of tissues (Fieni 2012. *Nat Commun*).

Here we tested the hypothesis that mtCU distribution is strategically biased towards mito-SR associations in the heart to support effective excitation-bioenergetics coupling.

RESULTS

1. Colocalization of MCU and RyR2 in adult mouse cardiomyocytes

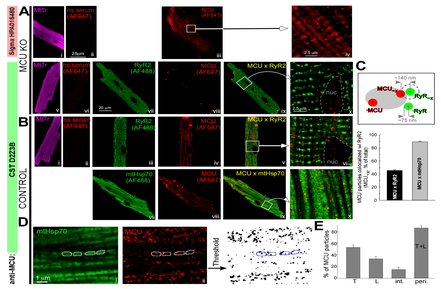

Anti-MCU and anti-RyR2 IF labeling of primary mouse cardiomyocytes (Zeiss LSM880 Airyscan super-resolution images). **A.** Validation of two anti-MCU antibodies (Sigma and Cell Signaling as labeled on the left edge) for IF in primary adult mouse cardiomyocytes lacking MCU (MCU KO). Negative control (no primary Ab) along with the mitochondrial (MitoTracker Red, MtTr) distribution is show on the left. **B. I**mages from control adult myocytes labeled with MCU&RyR2 or MCU&mtHsp70**. C.** Scheme for the colocalization analysis super-resolution images. The fluorescent spot size for the IF-labeling is ~150 nm with the Airy-scan super-resolution approach. The bar graphs show the % of MCU colocalized with RyR2 IF at 65nm distance. Note that this percentage (>45%) is higher than what random distribution would predict (<34%). **D**.MCU IF particle distrubution was analyzed with reference to masks drawn over individual mitochondria. Thresholded MCU particles over each mask were classified according to weather or not they contacted the contour and if they contacted the transversal or longitudinal contour side. Bar chart in **E** is summarizing the analysis. Note the higher frequency of particles at the transversal side despite the elongated shape.

2. MCU and RyR2 IF colocalization resolved by single-molecule super-resolution microscopy

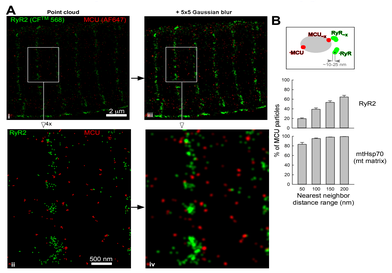

A. Mouse adult cardiomyocites were labeled with anti-MCU and anti-RyR2 and imaged using a Vutura 352 Super-Resolution System. Point cloud images are shown without further processing (left panels) or after applying a 5x5 gaussian blur filter (right panels). **B**. Co-localization (proximity) analysis between MCU and RyR2 IF and between MCU and mtHsp70 based on nearest neighbor distance ranges. The scheme illustrates approximate particle sizes.

3. Ca^{2+} signaling activity promotes MCU recuitment to dyad (RyR2) areas.

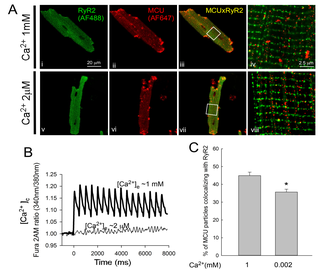

Colocalization of MCU and RyR2 fluorescence was determined in adult cardiomyocytes that were perfused with (1 mM) or quasi without (2 µM) Ca^{2+} and field-stimulated for 10 min (2Hz) before fixation. **A**. Airyscan images of MCU and RyR2 IF in representative cardiomyocytes (extracellular Ca^{2+}, $[Ca^{2+}]_e$ ~1 mM on top, ~2 µM at the bottom). **B**. Representative $[Ca^{2+}]_c$ recordings from two cardiomyocytes paced at $[Ca^{2+}]_e$ ~1mM or ~2 µM. **C**. Percent of MCU IF colocalization with RyR2.

4. Ultrastructural differences between SR and mitochondrial fractions.

Fewer mitochondria, less IMM integrity but more RyR2 associations in SR

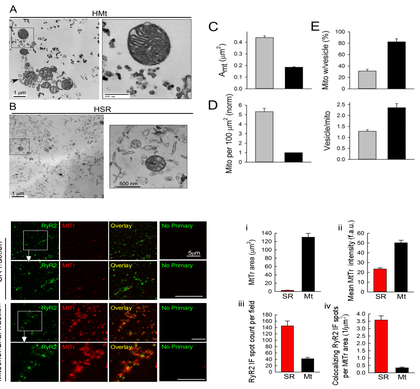

Membrane particles from the mitochondrial and SR fractions isolated from rat are compared **A-E**.TEM images of the organelles, membrane vesicles/particles in sections of high-pressure-frozen suspensions of Mt (**A**) and SR (**B**). Bar graphs show the average individual cross-section area **(C)** and quantity (count/100 mm^2) **(D)** of well-defined mitochondria from two independent preparations as well as the frequency of mitochondria-vesicle associations along with its extent (vesicle/mito) **(E). F.** Anti-RyR2 IF and MtTr distribution in glass-mounted SR and mitochondrial fractions. Bar graphs show the MtTr fluorescence area per field, the mean intensity of MtTrRed (loading is $\Delta\Psi_m$-dependent), the number of RyR2 IF spots per field as well as per area unit of (colocalizing) MtTr. While there are ~4x more RyR2 spots in the SR, the number of colocalizing RyR2 spots per MtTr area unit is disproportionally (>10 fold) higher in the SR

5. Comparison of the mitochondrial content in SR and Mitochondrial fractions.

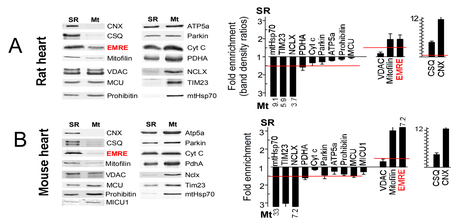

Crude heart SR fraction (SR, 45,000*g p___ mitochondrial pellet) is "contaminated" with mitochondrial fragments or small mitochondria that are presumably extensively associated with SR. If mtCU was biased towards mito-SR associations these mitochondria in SR would be particularly rich in mtCU constituents. **A.** WBs of various mitochondrial and SR resident proteins in rat SR and mitochondrial fractions. Bar graphs show the relative enrichment of the respective proteins in the mitochondrial and SR fractions, expressed as fold ratio of the WB band densities. The value of 1 would represent equal band densities between Mt and SR. **B** Is the same as **A** in mouse.

6. Percoll purification decreases MCU and EMRE levels in the mitochondrial fraction.

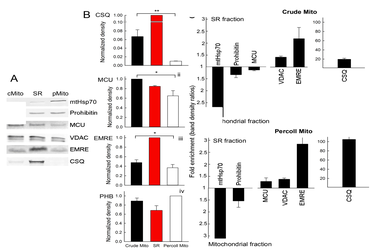

Mitochondrial and SR protein levels were compared between crude and percoll-purified mitochondrial fraction as well as the SR fraction isolated from rat heart. **A**. Representative WBs of mitochondrial and SR resident proteins in the three fractions as labeled (cMt and pMt are crude and percoll purified mitochondrial fractions respectively). **B**. Bar charts showing the the relative abundance of the SR resident calsequestrin and the mitochondrial proteins MCU, EMRE and prohibitin. **C.** Fold enrichment for all proteins analyzed in SR vs. crude mitochondrial and SR vs. percoll-purified mitochondrial fractions expressed as abundance ratios like in Fig. *6*

7. MCU and EMRE content profiles of differently sized protein complexes of mitochondrial and SR fractions.

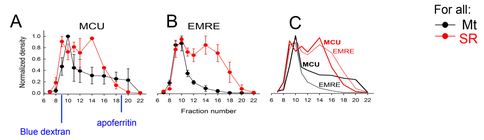

Protein complexes were separeted via size-exclusion (Sephacryl S400 HD) chromatography from non-denaturing detergent (CHAPS) lysates of Mitochondrial and SR fractions. The smaller the fraction number the larger is the size of the complexes. Abundances of MCU (**A**) and EMRE (**B**) proteins in the fractions determined by WB and normalized to the band intensity range. Line plots from B,C are overlaid in (**C**). EMRE follows MCU throughout the size range in SR but not in Mt, where it is un- or underrepresented in the smaller complexes.

8. Greater mitochondrial Ca^{2+} uptake efficacy in SR than in mitochondrial fractions

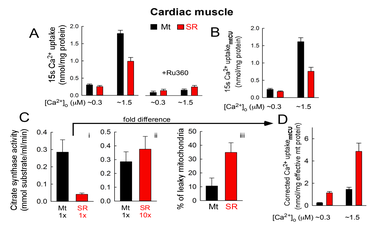

Ca^{2+} uptake assays based on $^{45}Ca^{2+}$ isotope retention. Ca^{2+} uptake activation was determined from the initial (15 s) $^{45}Ca^{2+}$ accumulation in suspensions of mitochondrial (Mt) and SR fractions of cardiac (**A-D**) muscle. SR Ca^{2+} store was depleted and SR Ca^{2+} uptake, mitochondrial Ca^{2+} extrusion pathways (mitochondrial Na^+/Ca^{2+} exchanger and the permeability transition pore) were pharmacologically blocked (respectively by thapsigargin, CGP-37157 and cyclosporine A). **A.** Initial Ca^{2+} uptake at $[Ca^{2+}]_0$ ~0.3 and ~1.5 mM in the absence and presence of Ru360 (10 µM) in cardiac mitochondrial and SR fractions. **B.** mtCU-mediated (Ru360 sensitive) initial Ca^{2+} uptake (Ca^{2+} $uptake_{mtCU}$) calculated from (**A**). **C**. Citrate synthase activity in the mitochondrial and SR fractions at equal protein amount per assay (left panel) or, for reference, with 10 times more unaltered protein in the SR than in the mitochondrial fraction. Right panel shows the percent portion of citrate synthase activity in the two fractions that did not require membrane permeabilization, corresponding to mitochondria with compromised IMM integrity ("leaky/broken mitochondria"). **D.** Initial Ca^{2+} $uptake_{mtCU}$ adjusted by the fold difference in citrate synthase activity per total protein between the mitochondrial and SR fractions (from **C**, as the arrow shows). Note that, after the correction, the mtCU mediated Ca^{2+} uptake is considerably higher in the SR than in the mitochondrial fraction.

Acknowledgements:

- **Grant support: R01 HL122124-01 to GC and SSS**
- **Grant support: AHA postdoctoral fellowship 16POST27770035 to SF**
- High-pressure freezing and freeze-substitution were done in the University of Pennsylvania Electron Microscopy Resource Laboratory core.

9. Na^+ dependent Ca^{2+} extrusion is weaker in the SR fraction than in the mitochondrial fraction

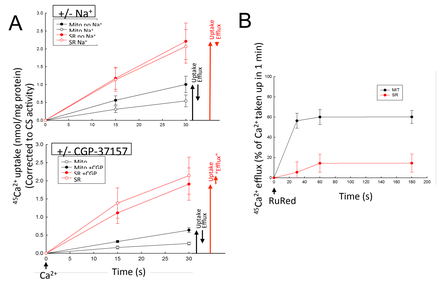

To determine the Na+-dependent Ca2+ extrusion capacity of the mitochondrial and SR fractions 45Ca2+ retention assays was performed. A. 45Ca2+ uptake was measured with or without inhibiting of the mitochondrial Na+/Ca2+ exchanger 15 and 30s after Ca2+ addition. The Ca2+ retention at inhibited Ca2+ extrusion (-Na+ or +CGP) reflects the uptake while the difference between +/- inhibition reflects the Ca2+ efflux as shown by the arrows on the right. Note that the efflux is more efficient in the Mitochondrial fraction than in the SR fraction. B. measurements of the Ca2+ extrusion directly by measuring the decrease in Ca2+ retention at the indicated time points after suspending 45Ca2+ uptake by the uniporter inhibitor Ruthenium red (RuRed, 3 mM). Note the much larger fractional decrease in the 45Ca2+ retention in the mitochondrial fraction.

CONCLUSIONS

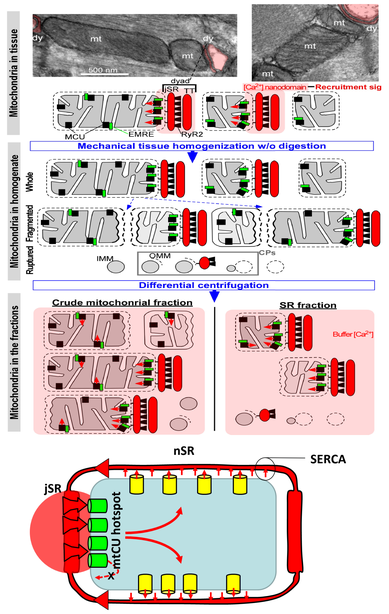

1. **In the heart mitochondria, the Ca^{2+} uniporter shows a biased distribution toward the dyadic SR interface areas. This preferential/ strategic distribution is conditioned by the exposure to Ca^{2+} signaling activity.**
2. **MCU and EMRE reside in complexes of a wide size range.**
3. **The molecular composition of the mtCU complex is heterogeneous in the cardiac mitochondria. EMRE that is essential for channel function is highly concentrated to SR. Outside the SR association areas some MCU-containing complexes are deprived of EMRE, and are likely functionally silent.**
4. **Na+-dependent extrusion seem to have a "cold spot" at the interface with dyadic SR. The respective hot and cold spots for Ca2+ uptake and extrusion would serve to optimize the efficacy of receiving Ca2+ signals at the dyadic interface and of feeding back the uptaken Ca2+ to the SERCA pumps in the network SR.**